Modern Aspects of Electrochemistry 57

Stojan Djokić *Editor*

Electrodeposition and Surface Finishing

Fundamentals and Applications

Springer

MODERN ASPECTS OF ELECTROCHEMISTRY

No. 57

Series Editors:
Ralph E. White
Department of Chemical Engineering
University of South Carolina
Columbia, SC 29208

Constantinos G. Vayenas
Department of Chemical Engineering
University of Patras
Patras 265 00
Greece

For further volumes:
http://www.springer.com/series/6251

Previously from Modern Aspects of Electrochemistry

Modern Aspects of Electrochemistry No. 55

Biomedical Applications

Edited by Stojan S. Djokić, Professor of Chemical & Materials Engineering at the University of Alberta

Topics in Number 55 include:

- CoCrMo alloy for biomedical applications
- Electroless synthesis of metallic nanostructures for biomedical technologies
- Biodegradable Mg alloys: Corrosion, surface modification and biocompatibility
- Microcantilever sensors: Electrochemical aspects and biomedical applications
- Surface treatments with silver and its compounds for biomedical applications

Modern Aspects of Electrochemistry No. 56

Applications of Electrochemistry in Medicine

Edited by Mordechay Schlesinger, Professor Emeritus, Department of Physics, University of Windsor, Canada.

Topics in Number 56 include:

- Electrochemistry in the design and development of medical technologies and devices
- Medical devices at the interface of biology and electrochemistry
- Sensing by screen printed electrodes for medical diagnosis
- Electrochemical glucose sensors
- Electrochemistry of adhesion and spreading of lipid vesicles on electrodes
- Bio-Electrochemistry and chalcogens
- Nanoplasmonics in medicine
- Extravascular hemoglobin: aging contusions
- Modeling tumor growth and response to radiation

Stojan S. Djokić
Editor

Electrodeposition and Surface Finishing

Fundamentals and Applications

Springer

Editor
Stojan S. Djokić
Elchem Consulting Ltd.
Edmonton, AB, Canada

ISSN 0076-9924 ISSN 2197-7941 (electronic)
ISBN 978-1-4939-0288-0 ISBN 978-1-4939-0289-7 (eBook)
DOI 10.1007/978-1-4939-0289-7
Springer New York Heidelberg Dordrecht London

Library of Congress Control Number: 2014932043

Printed on acid-free paper

Springer is part of Springer Science+Business Media (www.springer.com)

Dedicated to John O'M. Bockris
and Brian E. Conway

Preface

The series *Modern Aspects of Electrochemistry* has presented new developments in Electrochemistry since its inception in the early 1950s. This prestigious series contains works of many distinguished electrochemists worldwide including those of the series founders, Professors John O'M. Bockris and Brian E. Conway. The vision of Professors Bockris and Conway continues to achieve greatness with its 57th volume thanks to Springer and Dr. Kenneth Howell. I would especially like to point out that I was blessed with opportunities to study, work with, and collaborate with Professors Conway and Bockris. I owe a great deal to these two fine individuals for all I have learnt in the field of electrochemistry. Professors Bockris and Conway collaborated with many electrochemistry groups around the globe. In this way, Professors Bockris and Conway significantly influenced many electrochemists and developments in the electrochemical science and technology. I would especially like to mention the contributions of my former teacher, Professor Konstantin I. Popov, and his coworkers, who in spite of very limited equipment and finances are still achieving first class results.

This volume of *Modern Aspects of Electrochemistry* is devoted to Professors John O'M. Bockris and Brian E. Conway. Although Professor Brian E. Conway passed away in 2005 and Professor John O'M. Bockris, just recently, in July of 2013, their vision continues and will continue in the future. Significant contributions to this volume have come from individuals who were in one or another way influenced by these fine minds.

Chapter 1 by Jović et al. describes the electrodeposition of alloys and composite materials. After a historical overview of the early work, the chapter discusses the conditions for the electrodeposition of alloys from a thermodynamic point of view. The narrative then further explores the characterization of the electrodeposited alloys by electrochemical techniques. Anodic linear sweep voltammetry for the characterization of the electrodeposited alloys, e.g., eutectic, solid solution, and alloys with intermediate phases or intermetallic compounds is described and referenced in detail. In addition, the results of the analysis of electrodeposited alloys by the anodic sweep voltammetry are compared to those obtained by the X-ray diffraction. Finally, the chapter describes electrodeposition of composite

materials and their mechanical and electrical properties. Important discussion is devoted to the electrodeposition of Ni–MoO_2 composite coatings as cathodes for hydrogen evolution in industrial electrolysis.

In Chap. 2, Nikolić and Popov discuss the mechanistic aspects of lead electrodeposition. Electrodeposition of lead is characterized by a relatively high exchange current densities. For a while, it was generally accepted that the electrodeposition of lead proceeds in the whole range of overpotentials and that it is diffusion controlled. The experimental results and discussion in this chapter show that electrodeposition of lead may proceed under the conditions of pure ohmic or mixed ohmic-diffusion control. The conditions for lead electrodeposition are influenced by the concentration of Pb(II) in the solution. At higher concentrations of Pb(II) in the solution, electrodeposition of lead is completely under ohmic control. The surface morphology of the electrodeposited lead is determined by the conditions of electrodeposition. While under ohmic control well-defined single crystals of lead are produced, elecetrodeposition under mixed ohmic-diffusion control leads to the formation of dendritic deposits. The formation of different shapes of dendrites of lead during the electrodeposition is further attributed to the composition of the electrolytes used in the experiments. The primary type of dendrites is produced from the simple electrolytes, while the secondary type is formed from *complexed* solutions.

In Chap. 3, Mišković-Stanković discuses the electrophoretic deposition of ceramic materials onto metal surfaces. Ceramic coatings may be useful as anticorrosion surfaces or in biomedical applications as implants. Materials presented in this chapter include alumina, boehmite, monetite, brushite, hydroxyapatite, and their combination with silver and/or lignin. The effects of the parameters of electrochemical deposition on the thickness, morphology, and structure of the deposited ceramic coatings are discussed in this chapter. Various instrumental methods are used to describe the properties of electrodeposited ceramic coatings.

Chapter 4 by Tsui and Zangari reviews the fundamentals of the electrodeposition of metal oxides for the energy conversion and storage technologies. Electrochemical growth of oxide materials and methods to control their composition, surface morphology, and crystal structure in relation to the applications for the energy conversion are discussed. The materials examined in this chapter include ZnO for solar cells, Cu_2O for photovoltaic and photoelectrochemical systems, α-Fe_2O_3 for photoelectrochemical water splitting, and MnO_2 for the supercacitor energy storage.

Chapter 5 by Stojadinović et al. is devoted to the anodization of aluminum and more particularly to an interesting phenomenon—namely, luminescence—occurring during this process. While the anodization of aluminum has been investigated for quite some time, little or no attention has been paid to the occurrence of so-called galvanoluminescence, an emission of weak optical radiation, mostly in the visible spectrum. The nature of the galvanoluminescence depends on the electrolytes used in the process, surface pretreatment, and anodizing conditions. As such, the galvanoluminescent methods are recommended for use in the determination of the oxide film thickness, growth rate, refraction index, optical constants of alumina, etc. Anodization of aluminum above the breakdown voltage

leads to the formation of plasma as indicated by the presence of sparks on the surface, accompanied by the simultaneous gas evolution. As a consequence, the total luminescence increases. The spectroscopy analysis of plasma allows the determination of electron temperature and electron number density.

In Chap. 6, Cadian et al. analyze the electrochemical aspects of chemical and mechanical polishing. This process is widely used in the semiconductor manufacturing in order to generate complex three-dimensional geometries. A successful polishing of metals is based on the formation of a passive surface film. Chemical mechanical polishing performed on both tungsten and copper and the electrochemical interactions with the polishing slurry are discussed in this chapter. Electrochemical processes that lead to undesirable phenomena such as pitting, etching of the metal surface, galvanic corrosion, and re-deposition of material onto the polished surface are described in detail.

Chapter 7 by Djokić and Magagnin reviews the surface treatments prior to metallization of semiconductors, ceramics, and polymers. Classical and recently developed methods such as treatment of the ceramic and polymer surfaces with Pd (II) and Ag(I), as well as galvanic displacement reactions for the case of semiconductors, are discussed. Metallization of nonconductive surfaces is very important for many industrial applications.

I sincerely hope that this volume of the *Modern Aspects of Electrochemistry* will bring to scientists, researchers, engineers, and students review chapters related to the latest findings in the field of electrodeposition and surface finishing, The ideas discussed will have significant import for electronics, aerospace, automotive, energy devices, and biomedical applications.

Edmonton, AB, Canada Stojan S. Djokić

Contents

Contributors

Ivan Belča Faculty of Physics, University of Belgrade, Belgrade, Serbia

K. Cadien Department of Chemical and Materials Engineering, University of Alberta, Edmonton, AB, Canada

K. Dawkins Department of Chemical and Materials Engineering, University of Alberta, Edmonton, AB, Canada

Stojan S. Djokić Elchem Consulting Ltd, Edmonton, AB, Canada

B.M. Jović Department of Materials Science, Institute for Multidisciplinary Research, Belgrade, Serbia

V.D. Jović Department of Materials Science, Institute for Multidisciplinary Research, Belgrade, Serbia

Bećko Kasalica Faculty of Physics, University of Belgrade, Belgrade, Serbia

U.Č. Lačnjevac Department of Materials Science, Institute for Multidisciplinary Research, Belgrade, Serbia

Luca Magagnin Dipartimento di Chimica, Materiali e Ingegneria Chimica 'Giulio Natta', Politecnico di Milano, Milano, Italy

Vesna B. Mišković-Stanković Faculty of Technology and Metallurgy, University of Belgrade, Belgrade, Serbia

Nebojša D. Nikolić ICTM-Institute of Electrochemistry, University of Belgrade, Belgrade, Serbia

L. Nolan Portland Technology Development, Intel Corporation, Hillsboro, OR, USA

H. Pirayesh Department of Chemical and Materials Engineering, University of Alberta, Edmonton, AB, Canada

Konstantin I. Popov ICTM-Institute of Electrochemistry, University of Belgrade, Belgrade, Serbia

Faculty of Technology and Metallurgy, University of Belgrade, Belgrade, Serbia

Stevan Stojadinović Faculty of Physics, University of Belgrade, Belgrade, Serbia

Lok-kun Tsui Department of Materials Science and Engineering, University of Virginia, Charlottesville, VA, USA

Rastko Vasilić Faculty of Physics, University of Belgrade, Belgrade, Serbia

Z. Xu Department of Chemical and Materials Engineering, University of Alberta, Edmonton, AB, Canada

Giovanni Zangari Department of Materials Science and Engineering, University of Virginia, Charlottesville, VA, USA

Ljubiša Zeković Faculty of Physics, University of Belgrade, Belgrade, Serbia

Chapter 1
Electrodeposition and Characterization of Alloys and Composite Materials

V.D. Jović, U.Č. Lačnjevac, and B.M. Jović

1.1 Introduction

It is general experience in materials science that alloy can exhibit qualities that are unobtainable with parent metals. This is particularly true for electrodeposited alloys. Some important properties of materials, such as hardness, ductility, tensile strength, Young's modulus, corrosion resistance, solderability, wear resistance, and antifriction service, may be enhanced. At the same time some properties that are not characteristic for parent metals, such as high magnetic permeability, other magnetic and electrical properties, amorphous structure, etc., can also be obtained. In some cases alloy coatings may be more suitable for subsequent electroplate overlayers and conversion chemical treatments [1].

Some alloys may be more easily obtained by electrodeposition than by metallurgical processes. This is particularly true for alloys composed of metals having large differences in melting temperatures or cannot be mixed in a liquid state. Such metals can very often be codeposited from the solutions (e.g., alloys Ag–Ni, Ag–Co, and Cd–Co). Taking into account that some metals cannot be deposited from the aqueous solutions (Ti, V, W, Nb, Zr, etc.), they could be deposited from the melts of their salts. In recent times the processes of metals and alloys deposition from the room temperature molten salts were also investigated and developed (deposition of Al–Cu, Al–Co, Al–Ni alloys from $AlCl_3$–MeEtImCl melt).

The fast-growing requirements of modern industry for materials with special qualities in the last century have given rise to increasing interest in electrodeposition of alloys, particularly in corrosion protection and in the modern electronic industry [1].

V.D. Jović (✉) • U.Č. Lačnjevac • B.M. Jović
Department of Materials Science, Institute for Multidisciplinary Research,
Kneza Višeslava 1, 11030 Belgrade, Serbia
e-mail: vladajovic@imsi.rs

S.S. Djokić (ed.), *Electrodeposition and Surface Finishing: Fundamentals and Applications*, Modern Aspects of Electrochemistry 57,
DOI 10.1007/978-1-4939-0289-7_1,

Historically, the electroplating of alloys is practically as old as electroplating of pure metals, since the electroplating of brass and bronze was performed by De Ruolz [2] in 1842, shortly after the discovery of the first cyanide baths. It is interesting to note that these baths were essentially similar to ones used nowadays, being based on the use of Cu, Sn, and Zn complexes with cyanide.

From 1842 until the end of the nineteenth century, over 180 alloys involving 40 elements have been deposited [3]. An excellent review of the achievements up to 1962 is given in the book of Brenner [4], while from practical point of view it is recommended to consider the book of Bondar, Grimina, and Pavlov [5], which contains recipes and references for more than 1,100 baths for alloy deposition.

Although the first alloys [2] were deposited in 1842, practically the first attempt at scientific approach to electrodeposition of alloys, discussing the role of cathodic potential in the deposition of brass, came rather late with the work of Spitzer [6] in 1905. In 1914 a more comprehensive attempt came from Schlötter [7], but better under-standing of the alloy deposition process by understanding the electrochemical thermodynamics and kinetics, as well as complexometry and some other fields in order to obtain clear scientific bases, had to await second part of the nineteenth century. Some attempts were made by Gorbunova and Polukarov [8], Fedoteev et al. [9], and Faust [10], but they remained at a rather elementary level, obviously oriented to help practical electroplaters.

The results obtained until 1995 are summarized in the chapter by Despić and Jović [1]. Recently, published results on electrodeposition of alloys, with a particular attention on Ni–MoO_2 composite coatings used as catalysts for the hydrogen evolution reaction (HER), are discussed in this chapter.

1.2 Electrodeposition of Alloys from Aqueous Solutions

1.2.1 Conditions for Electrodeposition of Alloys

The metals immersed in the solution of their simple salts establish the reversible potential. The values of the reversible potentials for different metals could differ for about 3 V. Electrodeposition of metals could take place only at potentials more negative than the reversible ones. Accordingly, in the solution of ions of two metals (cf. Cu^{2+} and Zn^{2+}) with one being on the positive side of the potential scale (vs. SHE) (Cu) and another one being on the negative side of the potential scale (Zn), intensive deposition of Cu could take place at potentials at which Zn would not deposit at all. Taking into account that the reversible potentials of metals could change with the presence of different anions in the solution (complexation of metal ions), and that the rates of electrodeposition of different metals are usually different, it is possible to achieve conditions for simultaneous deposition of these two metals [1].

For simultaneous deposition of two metals, A and B, their deposition potentials (E) must be identical, $E(\mathrm{A}) = E(\mathrm{B})$, i.e.,

$$E_\mathrm{r}(\mathrm{A}) + \eta(\mathrm{A}) = E_\mathrm{r}(\mathrm{B}) + \eta(\mathrm{B}), \tag{1.1}$$

where $E_\mathrm{r}(\mathrm{A})$ and $E_\mathrm{r}(\mathrm{B})$ are reversible potentials of metals A and B, while $\eta(\mathrm{A})$ and $\eta(\mathrm{B})$ correspond to the overpotentials needed for the deposition of these two metals. The reversible potential could be changed by the change of metal ions concentration in the solution and by the temperature of the solution and is defined by the Nernst's equation:

$$E_\mathrm{r}(\mathrm{A}) = E^\Theta(\mathrm{A}) + \frac{RT}{pF}\ln a(\mathrm{A}^{\mathrm{p}+}), \tag{1.2}$$

$$E_\mathrm{r}(\mathrm{B}) = E^\Theta(\mathrm{B}) + \frac{RT}{qF}\ln a(\mathrm{A}^{\mathrm{q}+}), \tag{1.3}$$

where $E^\Theta(\mathrm{A})$ and $E^\Theta(\mathrm{B})$ are standard potentials of metals A and B, a activities of corresponding metal ions in the solution, and p and q numbers of electrons to be exchanged during the process of metal deposition.

The condition defined by Eq. (1.1) could be accepted only as a first approximation, since the potential of the metal deposition is undefined quantity if the value of corresponding current density is not known. It appears that a better definition of the conditions for simultaneous deposition of two metals would be current density at which both metals deposit with approximately the same current density. More precisely, for two-components alloy to be deposited with the molar ratio of the more noble metal x and the less noble metal $(1 - x)$, assuming that the Faraday's low is obeyed, following relations should be fulfilled:

$$x = \frac{n_\mathrm{A}}{n_\mathrm{A} + n_\mathrm{B}} = \frac{\frac{j_\mathrm{A}}{p}}{\frac{j_\mathrm{A}}{p} + \frac{j_\mathrm{B}}{q}} \tag{1.4}$$

and

$$(1 - x) = \frac{n_\mathrm{B}}{n_\mathrm{A} + n_\mathrm{B}} = \frac{\frac{j_\mathrm{B}}{q}}{\frac{j_\mathrm{A}}{p} + \frac{j_\mathrm{B}}{q}}, \tag{1.5}$$

where n_A and n_B are numbers of moles of components A and B. Hence, the current density ratio for the deposition of these two metals should be defined as

$$\frac{j_\mathrm{A}}{j_\mathrm{B}} = \frac{p}{q}\frac{x}{(1 - x)}. \tag{1.6}$$

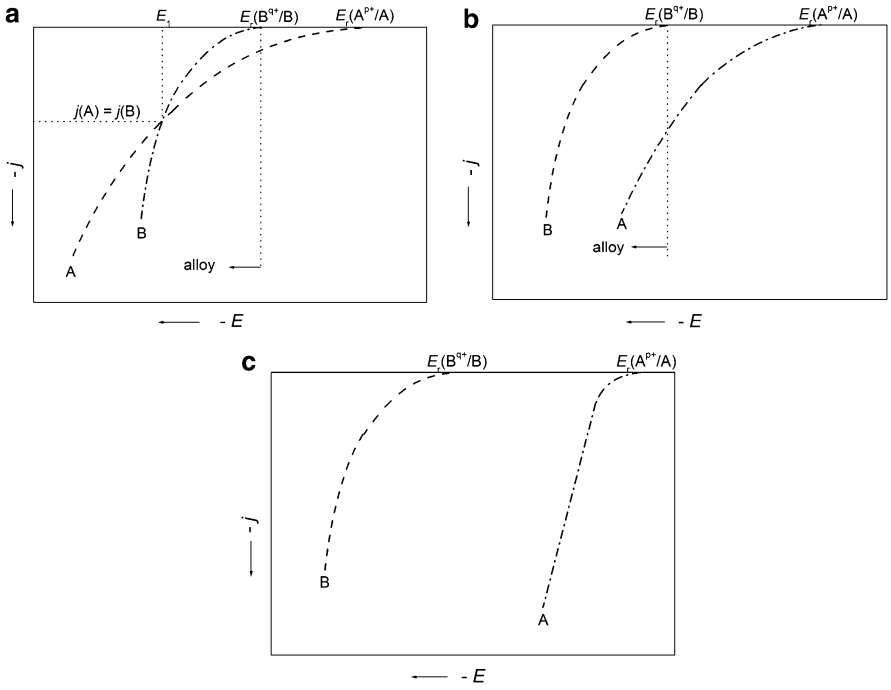

Fig. 1.1 Schematic presentation of the characteristic cases for alloy deposition

The condition defined by Eq. (1.6) could be achieved by proper adjustment of three essential variables: the concentration of the depositing ions at the electrode/solution interface (where the discharge occurs), the electrode potential, and the temperature.

In order to obtain better inside into the conditions defined by Eqs. (1.1, 1.2, 1.3, 1.4, 1.5, and 1.6), it is important to present polarization curves (current density versus potential relationships) for deposition of each metal. The characteristic cases are presented in Figs. 1.1 and 1.2. The first case is presented in Fig. 1.1a: the overpotential for deposition of the more noble metal A is higher than that for the less noble metal B. From the potentials $E_r(A^{p+}/A)$ to $E_r(B^{q+}/B)$ only more noble metal deposition occurs, while the deposition of alloy commences at the potential E_1. In the potential range from $E_r(B^{q+}/B)$ to E_1 metal A deposits with higher current density than metal B (the alloy contains more metal A than B). At the potential E_1 both metals deposit with the same current density, and the alloy contains the same amount of both metals. At the potentials more negative than E_1, the metal B deposits with higher current density and, accordingly, the alloy contains more metal B than metal A. The second case is presented in Fig. 1.1b: the overpotential for deposition of metal A is slightly lower than that for metal B, i.e., the polarization curves are almost parallel. Hence, the deposition of alloy commences at the potential $E_r(B^{q+}/B)$, while the alloy contains more metal A than B. If the difference between $E_r(A^{p+}/A)$ and $E_r(B^{q+}/B)$ is high and the overpotential for deposition of the

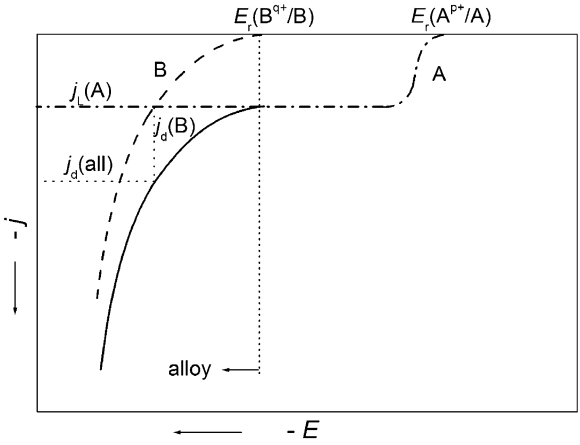

Fig. 1.2 Polarization curves for the deposition of more noble metal (A) and less noble metal (B): $j_L(A)$—diffusion limiting current density for the deposition of metal (A); $j_d(B)$—current density for the deposition of metal (B); $j_d(all)$—current density for the deposition of alloy

more noble metal A is lower than that for the less noble metal B, the third case, presented in Fig. 1.1c applies: in such a case alloy deposition is impossible. The difference between the reversible potentials of two metals could be changed (lowered) by the change of metal ions concentration (activity), and in most cases this is achieved by the complexation.

Simultaneous deposition of two metals is possible even if the difference in their reversible potentials is high if the applied current density for alloy deposition is higher than the diffusion limiting current density for the deposition of the more noble metal. Such a case is schematically presented in Fig. 1.2.

If $p = q = 2$ the molar ratios of metals (A) and (B) in the alloy are defined by the following relation:

$$x(\mathrm{A}) = \frac{j_\mathrm{L}(\mathrm{A})}{j_\mathrm{L}(\mathrm{A}) + j_\mathrm{d}(\mathrm{B})} = \frac{j_\mathrm{L}(\mathrm{A})}{j_\mathrm{d}(\mathrm{all})},$$
$$x(\mathrm{B}) = \frac{j_\mathrm{d}(\mathrm{B})}{j_\mathrm{L}(\mathrm{A}) + j_\mathrm{d}(\mathrm{B})} = \frac{j_\mathrm{d}(\mathrm{B})}{j_\mathrm{d}(\mathrm{all})}. \tag{1.7}$$

1.2.2 *Reversible Potential of Alloys in the Solution of Corresponding Ions*

According to the electroplating literature [4], when an alloy composed of metals A and B is immersed in the solution containing corresponding metal ions (A^{p+} and B^{q+}), its potential is termed as "static potential." In such a case it is desired to establish the conditions under which no net process would take place, so that the potential could be considered as the reversible potential of the alloy. Taking into account that an alloy may (and very often does) consist of several phases (intermetallic compounds), with each phase having different thermodynamic properties, it should be expected to have different reversible potential for each alloy composition. Such a case is essentially a

nonequilibrium situation. Nevertheless, the thermodynamic properties of each phase, and accordingly the problem of its reversible potential, can be treated assuming that this is the only phase present in a given situation (it will be discussed later).

The problem of the reversible potential of alloys has been treated in the literature [1, 11, 12] in terms of the Nernst equation applied to the less noble metal only, while the more noble component of the alloy being considered as an inert metal matrix. Such approach is not appropriate since it yields unrealistic results. Hence, in a proper approach the thermodynamic property of the alloy cannot be assigned to an individual component of the alloy. Instead, a phase should be treated as composed of a chemical entity of stoichiometric composition corresponding to the alloy composition. Accordingly, a phase can be described as $A_xB_{(1-x)}$ and the formation of one mole of the substance characterizing this phase should be presented by the following chemical reaction:

$$x\mathrm{A} + (1-x)\mathrm{B} \Leftrightarrow \mathrm{A}_x\mathrm{B}_{(1-x)}. \tag{1.8}$$

1.2.2.1 The Influence of the Gibbs Energy of Phase Formation

The change of the Gibbs energy in the formation of the phase $A_xB_{(1-x)}$ can be described in terms of their standard partial molar Gibbs energies (standard chemical potentials) as

$$\Delta_\mathrm{f}G^\Theta\left(\mathrm{A}_x\mathrm{B}_{(1-x)}\right) = \mu^\Theta\left(\mathrm{A}_x\mathrm{B}_{(1-x)}\right) - x\mu^\Theta(\mathrm{A}) - (1-x)\mu^\Theta(\mathrm{B}). \tag{1.9}$$

The phase $A_xB_{(1-x)}$ can also be formed in the electrochemical cell from the ions of both metals (A^{p+} and B^{q+}) present in the solution. In such a case the electrochemical cell is composed of an electrode made of the alloy phase as cathode and a standard hydrogen electrode as anode. The cell reaction is then

$$x\mathrm{A}^{\mathrm{p}+} + (1-x)\mathrm{B}^{\mathrm{q}+} + \left[\frac{xp+(1-x)q}{2}\right]\mathrm{H}_2 = \mathrm{A}_x\mathrm{B}_{(1-x)} + [xp+(1-x)q]\mathrm{H}^+. \tag{1.10}$$

The standard Gibbs energy change for this reaction is defined by the equation:

$$\begin{aligned}\Delta G^\Theta_\mathrm{cell} = {} & \mu^\Theta\left(\mathrm{A}_x\mathrm{B}_{(1-x)}\right) + [xp+(1-x)q]\mu^\Theta(\mathrm{H}^+) - x\mu^\Theta(\mathrm{A}^{\mathrm{p}+}) \\ & - (1-x)\mu^\Theta(\mathrm{B}^{\mathrm{q}+}) - \left[\frac{xp+(1-x)q}{2}\right]\mu^\Theta(\mathrm{H}_2).\end{aligned} \tag{1.11}$$

Taking into account that

$$[xp+(1-x)q]\mu^\Theta(\mathrm{H}^+) - \left[\frac{xp+(1-x)q}{2}\right]\mu^\Theta(\mathrm{H}_2) = 0, \tag{1.12}$$

it follows that the standard Gibbs energy change in the electrochemical cell is defined by the equation:

$$\Delta G^{\Theta}_{\text{cell}} = \mu^{\Theta}\left(\mathrm{A}_x\mathrm{B}_{(1-x)}\right) - x\mu^{\Theta}(\mathrm{A}^{\mathrm{p}+}) - (1-x)\mu^{\Theta}(\mathrm{B}^{\mathrm{q}+}). \tag{1.13}$$

The electromotive force of this cell, which is identical with the electrode potential of the alloy phase on the standard hydrogen scale, is given by

$$E\left(\mathrm{A}_x\mathrm{B}_{(1-x)}\right) = E^{\Theta}\left(\mathrm{A}_x\mathrm{B}_{(1-x)}\right) + \frac{RT}{[xp+(1-x)q]F}\ \ln\ a(\mathrm{A}^{\mathrm{p}+})^{x} a(\mathrm{B}^{\mathrm{q}+})^{(1-x)}. \tag{1.14}$$

The standard electrode potential of the alloy phase, $E^{\Theta}(\mathrm{A}_x\mathrm{B}_{(1-x)})$, is related to the standard Gibbs energy change in the cell, defined by the following equation:

$$\begin{aligned} E^{\Theta}\left(\mathrm{A}_x\mathrm{B}_{(1-x)}\right) &= \frac{-\Delta G^{\Theta}_{\text{cell}}}{[xp+(1-x)q]F} \\ &= \frac{-\mu^{\Theta}\left(\mathrm{A}_x\mathrm{B}_{(1-x)}\right) + x\mu^{\Theta}(\mathrm{A}^{\mathrm{p}+}) + (1-x)\mu^{\Theta}(\mathrm{B}^{\mathrm{q}+})}{[xp+(1-x)q]F}, \end{aligned} \tag{1.15}$$

where $[xp + (1 - x)q]F$ represents the total number of electrons exchanged in one act of the cell reaction [Eq. (1.10)].

The standard Gibbs energies of formation of the ions relative to that of the hydrogen ion (taken as zero), which are equal to the standard chemical potentials of the ions, are related to the standard potentials of the corresponding metals on the standard hydrogen scale as

$$\Delta_{\mathrm{f}} G^{\Theta}(\mathrm{A}^{\mathrm{p}+}) = \mu^{\Theta}(\mathrm{A}^{\mathrm{p}+}) = pFE^{\Theta}(\mathrm{A}^{\mathrm{p}+}/\mathrm{A}) \tag{1.16}$$

and

$$\Delta_{\mathrm{f}} G^{\Theta}(\mathrm{B}^{\mathrm{q}+}) = \mu^{\Theta}(\mathrm{B}^{\mathrm{q}+}) = pFE^{\Theta}(\mathrm{B}^{\mathrm{q}+}/\mathrm{B}). \tag{1.17}$$

Substituting Eqs. (1.16) and (1.17) into Eq. (1.15) and then substituting the resulting $E^{\Theta}(\mathrm{A}_x\mathrm{B}_{(1-x)})$ into Eq. (1.14), the reversible potential of the alloy phase is obtained as

$$\begin{aligned} E\left(\mathrm{A}_x\mathrm{B}_{(1-x)}\right) = {} & \frac{xp}{[xp+(1-x)q]}\left[E^{\Theta}(\mathrm{A}^{\mathrm{p}+}/\mathrm{A}) + \frac{RT}{pF}\ \ln\ a(\mathrm{A}^{\mathrm{p}+})\right] \\ & + \frac{(1-x)q}{[xp+(1-x)q]}\left[E^{\Theta}(\mathrm{B}^{\mathrm{q}+}/\mathrm{B}) + \frac{RT}{qF}\ \ln\ a(\mathrm{B}^{\mathrm{q}+})\right] \\ & - \frac{\mu^{\Theta}\left(\mathrm{A}_x\mathrm{B}_{(1-x)}\right)}{[xp+(1-x)q]F}, \end{aligned} \tag{1.18}$$

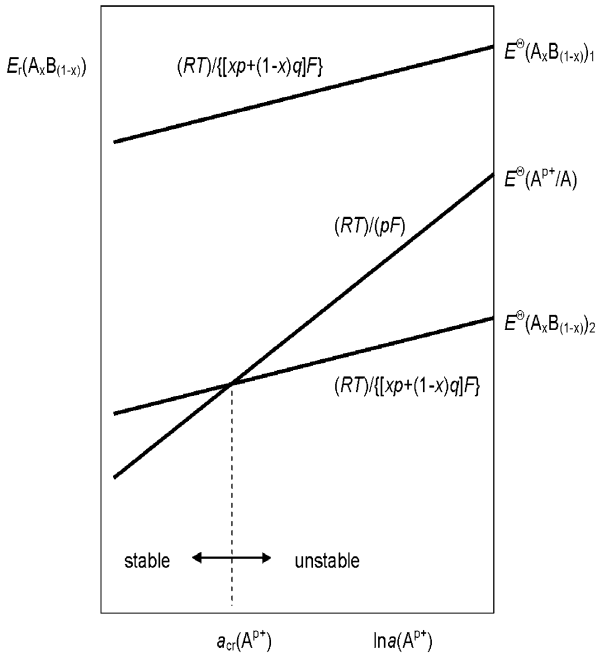

Fig. 1.3 Schematic presentation of the range of stability of phases $(A_xB_{(1-x)})_1$ and $(A_xB_{(1-x)})_2$ as a function of the concentration of more noble metal ions, ln $a(A^{p+})$ (Reprinted from [1] with the permission of Springer)

where $\mu^{\Theta}(A_xB_{(1-x)}) = \Delta_f G^{\Theta}(A_xB_{(1-x)}) - x\mu^{\Theta}(A) - (1-x)\mu^{\Theta}(B)$ is the standard chemical potential of the alloy phase relative to those of metal constituents. From Eq. (1.18) it could be concluded that: (a) the reversible potential of an alloy phase depends on the activities of ions of both metals in solution and (b) the dominant role in determining the position of the standard potential of the alloy phase relative to the pure metals is played by the standard molar Gibbs energy of the alloy phase formation [1].

1.2.2.2 Stability of Phases in the Solution of Corresponding Ions

When ions corresponding to metal constituents of an alloy phase are present in the solution, it is necessary to take into consideration their tendency to form other possible alloy phases or undergo reduction to pure metals. Accordingly, if another alloy phase or a pure metal would yield a more noble reversible potential, thermodynamic conditions for anodic dissolution of the existing alloy phase are created ("replacement reaction"). Hence, the considered alloy phase becomes unstable tending to undergo corrosive degradation. It can be shown that the instability depends on the activity of the metal ions in solution. Such a case [1] is schematically presented in Fig. 1.3.

Equation (1.14) defines the reversible potential of any alloy phase, as well as the reversible potential of the pure more noble metal ($x = 1$). Assuming a constant activity of the ions of the less noble constituent of the alloy ($a(B^{q+}) = 1$), it can be seen in Fig. 1.3 that the slope of a plot of E_r versus ln $a(A^{p+})$ is always larger for the pure more noble metal than for the alloy phase, since $\{x/[xp + (1 - x)q]\} < 1/p$ for any $x < 1$. If $E^{\Theta}(A_xB_{(1-x)})_1$ of the alloy phase 1 turns out to be more positive than other alloy phase 2, $E^{\Theta}(A_xB_{(1-x)})_2$, or of the pure more noble metal, $E^{\Theta}(A^{p+}/A)$, then the alloy phase will remain stable over the entire range of activities of ions of the more noble metal. If $E^{\Theta}(A_xB_{(1-x)})_2 < E^{\Theta}(A^{p+}/A)$, as shown in Fig. 1.3, there is a crossing point between the two functions at the activity $a_{cr}(A^{p+})$. At the activities larger than $a_{cr}(A^{p+})$ the metal would tend to precipitate on the account of dissolution of the alloy phase 2, i.e., the alloy phase 2 will be unstable. Conversely, at activities smaller than $a_{cr}(A^{p+})$ the alloy phase 2 will remain stable in the solution [1].

Taking into account discussion about the alloy phase stability, it is recommended not to introduce into the solution ions of the more noble metal, but only those of the less noble one. At the beginning of the nineteenth century (1907), Pushin [12] was aware of this fact and in his work the potentials of alloys were measured in the solution containing only less noble metal ions, and the same metal was used as the reference electrode.

1.2.3 Types of Electrodeposition of Alloys

According to Brenner [4], electrochemical codeposition of two metals to form an alloy could be: equilibrium, irregular, regular, anomalous, and induced. This classification is based on the relation between the composition of the deposited alloy (percentages of metals in the alloy) and the "metal ratio" which represents percentages of corresponding metal ions in the solution independently of their ionic form ("stoichiometric concentrations"). For the regular, irregular, and equilibrium codeposition, it is characteristic that the relative content of metals in the deposited alloy corresponds to that expected from the relation between their reversible potentials, whereas anomalous codeposition corresponds to the reverse situation. Induced codeposition is characteristic for the metals which cannot be deposited from the aqueous solutions, Mo, Ti, W, Ge, but can be codeposited with the iron-group metals (Fe, Co, Ni).

1.2.3.1 Equilibrium Codeposition

Equilibrium codeposition implies a common reversible potential for both metal constituents so that the reduction of both metal ions would take place at potentials more negative than the reversible ones. To close the gap between the reversible potentials of depositing metals, it is necessary to make the concentration of simple

salts (undergoing complete dissociation) of the more noble metal impractically low and of the less noble metal impractically high. As stated in Sect. 1.2.2.1 the best way to overcome this problem could result from complexation of metal ions with different ligands. Complexation usually changes the activity of the resulting species in solution by many orders of magnitude, while keeping the total amount of one or other metal in solution sufficiently high for a good supply of plating material to the cathode. It is very often case that the ions of both metals form complexes with one and the same ligand with similar values of the stability constants, so that the change of the potential of the deposition of each metal is the same (or similar) value. Usually, in such a case, the complexation with two different ligands could result in a more pronounced change of the deposition potentials of two metals. In a further text an example for the deposition of the Ni–Sn alloy from the solution containing pyrophosphate and glycine ligands is presented [13].

According to the literature [14] standard potential of the Ni deposition is −0.23 V vs. SHE, while that for Sn is −0.1364 V vs. SHE and accordingly Ni is less noble metal. Taking into account that the overvoltage for Ni deposition [15] is much higher than that for Sn deposition, the difference between the potentials of deposition of these two metals should be larger than that of their standard potentials. In the data presented in Dean's Handbook of Chemistry [16] Ni forms two pyrophosphate complexes, $[Ni(P_2O_7)]^{2-}$ and $[Ni(P_2O_7)_2]^{6-}$, and three glycine complexes, $[Ni(NH_2CH_2COO)]^{+}$, $[Ni(NH_2CH_2COO)_2]$, and $[Ni(NH_2CH_2COO)_3]^{-}$. There are only three papers in the literature with the data for different complexes of Ni and Sn in the pyrophosphate and glycine solutions, the data proposed by Duffield et al. [17], Turyan et al. [18], and Orekhova et al. [19]. Corresponding reactions for the formation of different complexes and their formation (stability) constants are given in the work of Duffield et al. [17]. All species and their stability constants used for the calculation of the distribution of different complexes in the solution containing Sn, Ni, pyrophosphate, and glycine ions are listed in Table 1.1.

The calculation of the distribution of complexes in the solution containing pyrophosphate and glycine showed that $[Sn(P_2O_7)_2]^{6-}$ is dominant complex with Sn at pH 8.0, while two complexes of Ni dominate: complex $[Ni(P_2O_7)_2]^{6-}$ and complex $[Ni(NH_2CH_2COO)_3]^{-}$. This is shown in Fig. 1.4.

The values of the equilibrium potentials of prevailing complexes (E_{eq}), calculated using explanations based on the Gibbs energy change for reaction of certain complex formation [20] (assuming that the ions activities are equal to their concentrations), are also presented in Table 1.1. As can be seen, the equilibrium potential for deposition of Sn by the reduction of $[Sn(P_2O_7)_2]^{6-}$ complex is −0.847 V vs. SCE, while the equilibrium potentials for the reduction of $[Ni(P_2O_7)_2]^{6-}$ and $[Ni(NH_2CH_2COO)_3]^{-}$ complexes are more positive, being about −0.716 V vs. SCE, and situation becomes opposite to that for deposition from the solution of simple ions. After the complexation Ni becomes more noble metal, while Sn becomes less noble one. Hence, it could be concluded that at pH 8.0 Sn would deposit from the complex $[Sn(P_2O_7)_2]^{6-}$, while Ni would deposit simultaneously from two complexes, $[Ni(P_2O_7)_2]^{6-}$ and $[Ni(NH_2CH_2COO)_3]^{-}$, in the presence of both complexing anions. The equilibrium potentials for deposition

Table 1.1 All complexes present in the solution containing 0.1 M $SnCl_2$ + 0.1 M $NiCl_2$ + 0.6 M $K_4P_2O_7$ + 0.3 M NH_2CH_2COOH, their concentrations, stability constants, and equilibrium potentials of prevailing complexes

Complexes	log β	Conc. (M)	E_{eq} (V vs. SCE)
$[H(P_2O_7)]^{3-}$	8.14		
$[H_2(P_2O_7)]^{2-}$	14.01		
$[H_3(P_2O_7)]^{-}$	15.78		
$[H_4(P_2O_7)]$	16.63		
$[H(NH_2CH_2COO)]$	9.64		
$[H_2(NH_2CH_2COO)]^{+}$	12.05		
$[Sn(NH_2CH_2COO)H]^{2+}$	12.78		
$[Sn(NH_2CH_2COO)]^{+}$	10.02		
$[Sn(P_2O_7)]^{2-}$	**13.05**	**0.007**	**−0.847**
$[Sn(P_2O_7)H]^{-}$	15.92		
$[Sn(P_2O_7)H_2]$	17.47		
$[Sn(P_2O_7)_2]^{6-}$	**16.27**	**0.093**	**−0.847**
$[Sn(P_2O_7)_2H]^{5-}$	22.31		
$[Sn(P_2O_7)_2H_2]^{4-}$	26.79		
$[Sn(P_2O_7)_2H_3]^{3-}$	30.07		
$[Sn(P_2O_7)_2H_4]^{2-}$	31.58		
$[Sn(P_2O_7)OH]^{3-}$	5.32		
$[Sn(P_2O_7)(OH)_2]^{2-}$	−4.77		
$[Sn(P_2O_7)_2OH]^{5-}$	7.04		
$[Ni(NH_2CH_2COO)]^{+}$	5.60		
$[Ni(NH_2CH_2COO)_2]$	**10.40**	**0.009**	**−0.716**
$[Ni(NH_2CH_2COO)_3]^{-}$	**13.80**	**0.057**	**−0.716**
$[Ni(P_2O_7)]^{2-}$	**5.80**	**0.005**	**−0.716**
$[Ni(P_2O_7)_2]^{6-}$	**7.40**	**0.029**	**−0.716**

Reprinted from [13] with the permission of Electrochemical Society

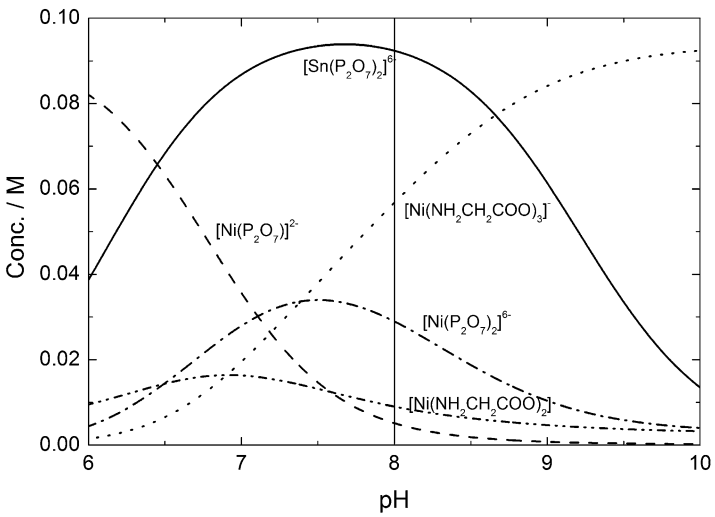

Fig. 1.4 Distribution of different complexes in the solution containing 0.1 M $SnCl_2$ + 0.1 M $NiCl_2$ + 0.6 M $K_4P_2O_7$ + 0.3 M NH_2CH_2COOH as a function of the solution pH

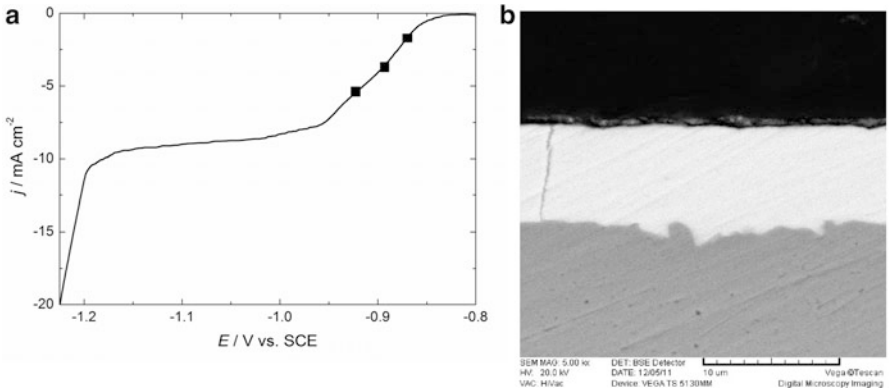

Fig. 1.5 (**a**) Polarization curve for deposition of the Ni–Sn alloy onto Ni electrode. (**b**) Typical cross section of coatings obtained at different current densities marked with solid squares in Fig. 1.5a (Reprinted from [21] with the permission of Int. J. Hydrogen Energy)

of Sn and Ni still differ for 0.131 V. As already stated, because of high overvoltage for Ni deposition [13], it could be expected that two metals possess identical, or similar, potential of deposition. This is exactly the case for these two metals in the pyrophosphate–glycine solution. The polarization curve for Ni–Sn alloy deposition onto Ni electrode is shown in Fig. 1.5a [21]. The deposition process commences at about −0.83 V vs. SCE being activation controlled down to about −0.95 V vs. SCE, while in the potential range from about −0.95 V to about −1.20 V well-defined diffusion limiting current density (−10 mA cm^{-2}) is established. In the region of the activation control (squares marked on Fig. 1.5a), Ni–Sn alloy coatings were deposited at the current densities of −2, −4, and −6 mA cm^{-2}. Flat and compact deposits were obtained in all cases, as shown in Fig. 1.5b. The composition of the coatings changed with the increase of cathodic current density from about 37 at.% Ni (for sample obtained at −2 mA cm^{-2}) to about 45 at.% Ni (for sample obtained at −6 mA cm^{-2}) [21], but in all cases both metals were present in the coating, indicating a good example for equilibrium codeposition.

1.2.3.2 Irregular Codeposition

The irregular type of codeposition is very often characterized by simultaneous influence of cathodic potential and diffusion phenomena, i.e., it mainly occurs under the activation and/or mixed control of the deposition processes. The rate of deposition in such a case is expressed by Butler–Volmer equation which is usually used for the kinetics of electrochemical processes [1]:

$$\frac{j}{j^{o}} = \frac{j_{o}}{j^{o}}\left[\exp\left(\frac{\alpha_{a}F}{RT}\eta\right) - \left(\frac{c}{c_{o}}\right)\exp\left(\frac{-\alpha_{c}F}{RT}\eta\right)\right], \tag{1.19}$$

where $\eta = E - E_{r}$ corresponds to the overpotential needed for the deposition of metals [see Eq. (1.1)], c and c_{o} represent concentrations of the discharging species at the surface of the electrode and in the bulk of the solution, respectively, j_{o} is "exchange current density" related to the rate constant of the deposition process, and α_{a} and α_{c} are anodic and cathodic transfer coefficients related to the mechanism of discharge (note that for a cathodic process both η and j acquire negative signs. Also note that the current densities are divided by arbitrarily chosen unit current j^{o} in order to obtain dimensionless values for further use).

If the discharge of depositing species is sufficiently slow so that their supply to the electrode surface occurs without difficulty, the concentration c virtually does not deviate from c_{o}, and such a case is termed "activation controlled" deposition with the rate-determining step being the activation energy of the discharge process. At any cathodic overpotential larger than −40 mV, the first term in Eq. (1.19) becomes negligible, so that this equation can be transformed into a simpler one, known as the Tafel equation:

$$\eta = a - b\log\left(-\frac{j}{j^{o}}\right), \tag{1.20}$$

where the Tafel constant a is

$$a = \frac{2.3RT}{\alpha_{c}F}\log\left(\frac{j_{o}}{j^{o}}\right), \tag{1.21}$$

while the slope of the linear dependence obtained from a plot η versus $\log(-j)$ (Tafel slope) is

$$b = \frac{2.3RT}{\alpha_{c}F}. \tag{1.22}$$

The above reasoning applies equally and independently to both metals (A) and (B), j_{A} and j_{B}, and the total current density being $j_{alloy} = j_{A} + j_{B}$.

It should be stated here that the concept of overpotential is related to the reversible potential of a pure metal in a given solution. In the case of codeposition of two metals and the formation of a phase $A_{x}B_{(1-x)}$, this potential has no physical meaning since it represents an arbitrary point to which j_{o} is related.

Typical cases of activation-controlled codeposition of the metals A (j_{A}) and B (j_{B}), presented as polarization curves for pure metals and an alloy phase (j), are shown in Fig. 1.6.

The Tafel functions, presented in Fig. 1.7, indicate linear relationships between the logarithm of the partial current densities and the electrode potential. When this

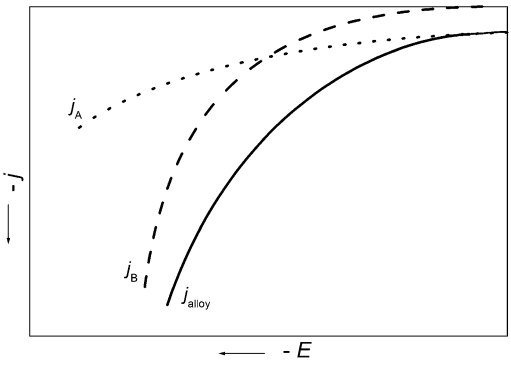

Fig. 1.6 Typical cases of activation-controlled codeposition of the metals A (j_A) and B (j_B), presented as polarization curves for pure metals and an alloy phase ($j_{alloy} = j_A + j_B$) (Reprinted from [1] with the permission of Springer)

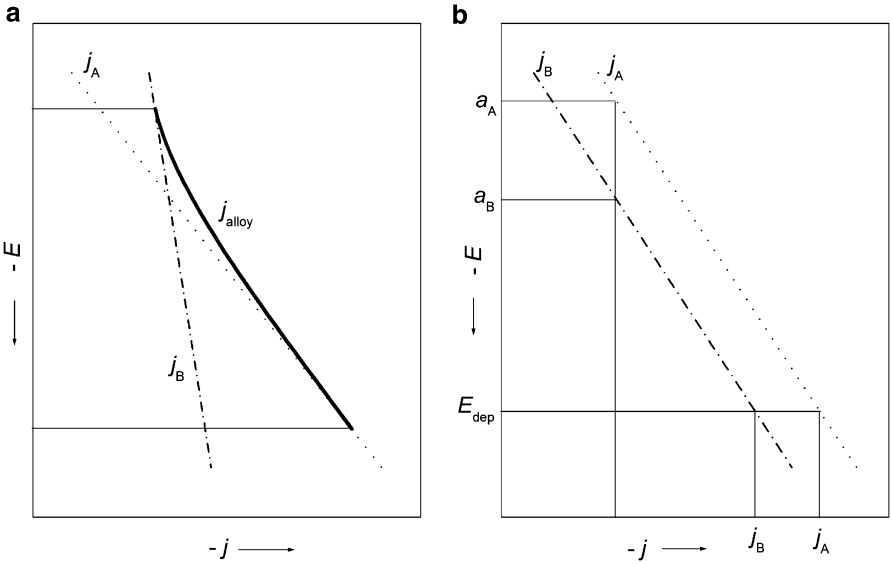

Fig. 1.7 Tafel functions for activation-controlled codeposition of the metals A (j_A) and B (j_B) and an alloy (j_{alloy}). (**a**) Different slopes of Tafel functions for pure metals deposition. (**b**) The same slopes of Tafel functions for pure metals deposition (Reprinted from [1] with the permission of Springer)

is the case, the total current density j_{alloy} cannot be a linear function of potential in the region in which the two partial current densities are comparable, since $\log (j_A + j_B) \neq \log j_A + \log j_B$ (Fig. 1.7a). When the Tafel function of the total current density merges with one or the other partial current density line, then one or the other metal is obtained virtually pure. In the extreme case in which the Tafel slopes for both depositing metals are equal, as shown in Fig. 1.7b, the difference between $\log j_A$ and $\log j_B$ remains constant, i.e., the composition of the alloy is constant at all potentials. In such a case the actual composition of the alloy depends on the difference between the values of the Tafel constants (a) for the two metals.

Considering the values of the Tafel constants and Tafel slopes, it is possible to analyze the factors determining the deviation of the metal ratio in the alloy from the metal ratio in solution. At any constant potential following relation is valid:

$$a_{\mathrm{A}} - b_{\mathrm{A}} \log\left(-\frac{j_{\mathrm{A}}}{j_{\mathrm{o}}}\right) = a_{\mathrm{B}} - b_{\mathrm{B}} \log\left(-\frac{j_{\mathrm{B}}}{j_{\mathrm{o}}}\right). \tag{1.23}$$

According to Eq. (1.6) one can derive:

$$\log\frac{x_{\mathrm{A}}}{x_{\mathrm{B}}} = \log\left(\frac{pj_{\mathrm{A}}}{qj_{\mathrm{B}}}\right) = \left[\left(\frac{a_{\mathrm{A}}}{b_{\mathrm{A}}} - \frac{a_{\mathrm{B}}}{b_{\mathrm{B}}}\right) - \left(\frac{b_{\mathrm{B}} - b_{\mathrm{A}}}{b_{\mathrm{A}} b_{\mathrm{B}}}\right)E\right]\frac{p}{q}. \tag{1.24}$$

Returning to the linear coordinates one obtains:

$$\frac{x}{1-x} = \frac{x_{\mathrm{A}}}{x_{\mathrm{B}}} = \frac{(j_{\mathrm{o}})_{\mathrm{A}} pa(\mathrm{A}^{\mathrm{p}+})^{(\alpha_{\mathrm{c}})_{\mathrm{A}}/p}}{(j_{\mathrm{o}})_{\mathrm{B}} qa(\mathrm{B}^{\mathrm{q}+})^{(\alpha_{\mathrm{c}})_{\mathrm{B}}/q}} \exp\left(\frac{RT}{F}\right) \left\{\left[(\alpha_{\mathrm{c}})_{\mathrm{A}} E^{\Theta}(\mathrm{A}^{\mathrm{p}+}/\mathrm{A}) - (\alpha_{\mathrm{c}})_{\mathrm{B}} E^{\Theta}(\mathrm{B}^{\mathrm{q}+}/\mathrm{B})\right] - \frac{(\alpha_{\mathrm{c}})_{\mathrm{A}} - (\alpha_{\mathrm{c}})_{\mathrm{B}}}{(\alpha_{\mathrm{c}})_{\mathrm{A}}^{\,2} (\alpha_{\mathrm{c}})_{\mathrm{B}}^{\,2}}\right\}. \tag{1.25}$$

Hence, it appears that the composition of the alloy follows a complex dependence on the metal ratio, involving all the thermodynamic and kinetic parameters determining activation-controlled codeposition [1].

As shown in Fig. 1.7 the Tafel lines are meant to pertain to the deposition of pure metals under the assumption that alloying does not change the Tafel constants and that the current density for alloy deposition should be a sum of partial current densities for pure metals. However, in practice, deviation from such behavior has been recorded, and an attempt to explain this phenomenon has been reported by Gorbunova and Polukarov [8] on an extreme case in which surface diffusion of A across the grains of B and nucleation of new grains of A are strongly inhibited.

An example for this type of alloy deposition is presented in Fig. 1.33 for the system Ag–Cd (cf. Sect. 1.3.3.3).

1.2.3.3 Regular Codeposition

Regular codeposition assumes transport-controlled codeposition in which diffusion of metal ions of both metals is a rate-determining step in the overall codeposition reaction.

Under steady state conditions of deposition the diffusion is governed by Fick's first law [22]: